Journal of Power Sources 243 (2013) 635–640

Contents lists available at SciVerse ScienceDirect

Journal of Power Sources

journal homepage: www.elsevier.com/locate/jpowsour

Novel O_2-enhanced methanol oxidation performance at Pt–Ru–C sputtered anode in direct methanol fuel cell

Sayoko Shironita, Masafumi Ueda, Yosuke Matsumoto, Minoru Umeda*

Department of Materials Science and Technology, Faculty of Engineering, Nagaoka University of Technology, 1603-1, Kamitomioka, Nagaoka, Niigata 940-2188, Japan

HIGHLIGHTS

- We successfully prepared Pt–Ru–C electrodes using a sputtering technique for the DMFC anode.
- The obtained Pt–Ru–C electrode undergoes an O_2-enhanced methanol oxidation in the H_2SO_4 solution.
- The O_2-enhanced methanol oxidation has been demonstrated in a DMFC single cell.
- The electrode can be used as an efficient DMFC anode by feeding a mixture of methanol and O_2.

ARTICLE INFO

Article history:
Received 16 April 2013
Received in revised form
26 May 2013
Accepted 12 June 2013
Available online 18 June 2013

Keywords:
Pt–Ru–C anode
Co-sputtering technique
O_2-enhanced methanol oxidation
Direct methanol fuel cell
Membrane electrode assembly

ABSTRACT

We have developed a novel anode catalyst for the direct methanol fuel cell (DMFC). A Pt–Ru–C electrode was prepared by a co-sputtering technique and compared with Pt and Pt–Ru sputtered electrodes for the methanol electro-oxidation reaction. The prepared Pt–Ru–C electrode with a specific atomic ratio showed a remarkable O_2-enhanced methanol oxidation performance by O_2 addition to methanol as a fuel. For practical utilization, the relationship between the O_2-enhanced methanol oxidation activity and the thermal stability of the Pt–Ru–C sputtered electrode was evaluated using a post-annealing treatment. It is found that the O_2-enhanced methanol oxidation activity of the Pt–Ru–C electrodes is retained if the annealing temperature is less than or equal to 100 °C. Finally, the DMFC performance was assessed using a single DMFC cell incorporating a membrane electrode assembly with Pt–Ru–C which was hot-pressed at 100 °C. The O_2-enhanced methanol oxidation was observed at a single DMFC cell also. Moreover, the enhanced reaction was recognized in DMFC power generation by feeding methanol and oxygen to the anode and oxygen to the cathode.

1. Introduction

The direct methanol fuel cell (DMFC) is a small, clean energy converter operated at low temperature, such as around room temperature. In this system, methanol supplied to the anode is directly oxidized. Therefore, no reforming equipment is needed, which leads to the realization of a compact and light-weight DMFC system. Based on this feature, the DMFCs are expected to be used as power sources for portable electronic devices [1]. However, the DMFC has not yet been widely used because of its low power density. With regard to the reasons for the low power density of the DMFCs, (i) a low methanol oxidation activity of the anode catalyst [2–5], and (ii) a decline in the O_2 reduction performance due to a methanol crossover [6] have been considered.

We have recently reported that the methanol oxidation performance at a Pt–C electrode prepared by co-sputtering is not influenced by O_2 addition [7]. To our surprise, the Pt–C electrode with a specific Pt:C atomic ratio shows an outstanding methanol oxidation performance, which is enhanced by the added O_2. This O_2-sensitized methanol oxidation performance can preferably be used for the DMFC anode. However, the onset potentials of the methanol oxidation (denoted as E_{onset}) at the Pt–C electrodes are not very negative in the presence of O_2 for effective operation in the DMFC.

It is generally accepted that the methanol oxidation at the Pt-based catalysts (Pt–M) occurs as follows [8–12]:

$$Pt + CH_3OH \rightarrow 4H^+ + Pt - CO_{ad} + 4e^-, \quad (1)$$

$$M + H_2O \rightarrow M - OH_{ad} + H^+ + e^-, \quad (2)$$

* Corresponding author. Tel./fax: +81 258 47 9323.
E-mail address: mumeda@vos.nagaokaut.ac.jp (M. Umeda).

0378-7753/$ – see front matter © 2013 Elsevier B.V. All rights reserved.
http://dx.doi.org/10.1016/j.jpowsour.2013.06.054

$$Pt - CO_{ad} + M - OH_{ad} \rightarrow CO_2 + 2Pt + H^+ + e^-, \quad (3)$$

in which, the rate-determining step of the methanol oxidation is believed to be Eq. (2) [12]. When the M is Pt, reaction (2) starts at 0.7 V vs. NHE [8,9], resulting in a comparatively positive E_{onset}. In contrast, when Pt is alloyed with Ru (the M is Ru), reaction (2) occurs at around 0.2 V vs. NHE [8,9], which leads to an E_{onset} shift to a negative potential. Based on this fact, the E_{onset} at the Pt–C electrode can be improved by replacing Pt with a Pt–Ru alloy.

In this study, we focused our attention on a Pt–Ru–C co-sputtered ternary system in order to realize the O_2-enhanced methanol oxidation reaction with a negative E_{onset}. The Pt–Ru–C ternary electrodes were prepared by a multi co-sputtering technique [13–16], which allows the preparation of a thin film not only on a flat Au substrate but also on a porous carbon paper. The electrocatalytic activity of the methanol oxidation reaction at the prepared Pt–Ru–C electrode was first measured in N_2- and O_2-saturated H_2SO_4 solutions. And the thermal stability for the O_2-enhanced methanol oxidation was also evaluated by preparing a membrane electrode assembly (MEA) by hot-pressing. Thereafter, the same type of methanol oxidation was measured at the MEA by changing the temperature. Finally, the DMFC power generation was assessed using a DMFC single cell incorporating the same MEA. The result of this study will be applied to the anode of a mixed reactant direct methanol fuel cell.

2. Experimental

2.1. Preparation of sputtered electrodes

Pt, Pt–Ru, and Pt–Ru–C thin-layer electrodes were prepared using a multi-target sputtering machine (ULVAC, CS-200) [7,13–15]. Pt and Ru disks, and two graphite carbon disks were used as the sputtering targets. The diameters of all the targets were 8 cm. An Au foil (8-mm diameter, 0.05-mm thickness) and a glassy carbon plate (10×10-mm^2 area, 1-mm thickness; Tokai Carbon, GC-20SS) were used as the sputter-deposition substrates for the electrochemical measurements. In addition, the Pt–Ru–C was sputter-deposited on a carbon paper (TGP-H-060H, Toray) substrate over a 5-cm^2 area for use as the MEA anode. Before the sputtering, these substrates were washed by ultrasonic agitation in acetone and then in Milli-Q water for 10 min each.

The experimental procedure for the sputter-deposition is described as follows. A rotating holder bearing the substrates was installed in a vacuum chamber, and the chamber was then evacuated by rotary and turbo-molecular pumps to a base pressure of 3×10^{-4} Pa. Subsequently, 99.999% Ar gas was introduced into the chamber to a pressure of 3 Pa; then the substrate was exposed to an inverse sputter-etching process to remove any residue on the surface. This pre-sputtering was conducted at the DC power of 200 W for 120 s. After the etching, Pt, Ru, and C were simultaneously sputtered onto the substrate under the conditions listed in Table 1, while the substrate holder was rotated at 10 rpm. During the sputtering, RF power was supplied to the Pt and Ru targets, and DC power was supplied to the C targets. After the sputtering, the pressure in the chamber was allowed to return to atmospheric pressure before the samples were removed. The formed Pt–Ru–C layer had a 5-mm diameter with a 50–100-nm thickness on the Au and glassy carbon and 2.3 cm $\times$ 2.3 cm on the carbon paper.

The MEA (geometric electrode area, 5 cm^2) used in this study was prepared as follows [16,17]. Nafion 117 (Dupont) was used as the polymer electrolyte membrane. The membrane (5 cm $\times$ 5 cm) was boiled in 0.5 mol dm^{-3} H_2SO_4 for 1 h and then washed twice by boiling in Milli-Q water for 1 h. The above-prepared Pt–Ru–C on carbon paper served as the anode. The total amount of Pt and Ru was adjusted to 1.0 mg cm^{-2}. A commercially available Pt/C (amount of deposited Pt: 45.9 wt. %, Tanaka Kikinzoku Kogyo Co., Ltd.) catalyst was used in the cathode. The Pt/C was dispersed using a ball mill in a 5 wt. % Nafion solution (Wako Pure Chemical Industries) diluted with a mixed solvent of methanol, 2-propanol, and Milli-Q water (1:1:1 weight ratio). The dispersed solution was spread on the carbon paper (TGP-H-060H, Toray) over a 5-cm^2 area. The amount of the spread Pt was adjusted to 1.0 mg cm^{-2}. Subsequently, the pretreated Nafion 117 membrane was sandwiched between the two catalyst-loaded carbon papers and then hot-pressed at 7.5 kN and 100 °C for 10 min.

Table 1
Sputtering conditions and Pt:Ru:C atomic ratios of co-sputtered electrodes.

Output power/W			Sputtering time[a]/min	Substrate	Atomic ratio of Pt:Ru:C[b]
Pt[c]	Ru[c]	C[d]			
100	0	0	30	Au	100:0:0
100	100	0	30	Au	78:22:0
50	120	500	30	Au	56:38:6

[a] Ar gas pressure and temperature were fixed at 3 Pa and room temperature, respectively.
[b] The atomic ratios were estimated by EDS.
[c] Pt and Ru were sputtered using RF power generators.
[d] C was sputtered using two graphite carbon target plates and a DC power generator.

2.2. Characterization of co-sputtered electrode

The atomic ratios of the co-sputtered electrodes were analyzed using an energy-dispersive X-ray analyzer (EDX: JEOL, JED-2300) combined with a scanning electron microscope (SEM: JEOL, JSM-6060A). The analyzed data are listed in Table 1. The crystal structures of the prepared electrodes were evaluated by X-ray diffraction (XRD: Shimadzu, XD-D1) at 30 mA and 30 kV using Cu-Kα radiation. The XRD patterns were measured in the range of $2\theta = 20$–80 degrees.

X-ray photoelectron spectroscopy (XPS) (JEOL, JPS-100SX) was conducted to investigate the electronic structure of the co-sputtered layer. Prior to the measurement, the sample surface was cleaned by Ar ion etching; then the XPS spectra were obtained using Mg-Kα radiation to induce excitation of the photoelectrons.

2.3. Electrochemical measurements in H_2SO_4 solution

The electrochemical properties of the sputter-deposited Pt, Pt–Ru, and Pt–Ru–C electrodes were evaluated using a three-compartment electrochemical cell. A supporting electrolyte of a 0.5 mol dm^{-3} H_2SO_4 solution was prepared by diluting concentrated H_2SO_4 (Wako Pure Chemical) with Milli-Q water. An Ag/Ag_2SO_4 [16,18–20] and a Pt coil were used as the reference and counter electrodes, respectively. The Pt, Pt–Ru, and Pt–Ru–C sputtered electrodes were used as the working electrodes and their potentials were controlled by a potentiostat (Hokuto Denko, HAB-151). All the electrochemical measurements were conducted at 25 ± 1 °C, and the electrode potentials in this report are referenced to the normal hydrogen electrode potential (NHE) at the same temperature. The measured currents were normalized by the geometric surface area (0.196 cm^2) of the sputtered electrode, which was exposed to the electrolytic solution.

The electrochemical measurements were conducted as follows. The sputtered electrodes were pretreated by potential cycling at the rate of 10 mV s^{-1} in N_2-saturated 0.5 mol dm^{-3} H_2SO_4 solution until the voltammogram was unchanged, so that the electrode surface

could be stabilized. The potential cycling was reversed from a cathodic sweep to an anodic sweep immediately before H_2 evolution, and the anodic sweep was conducted up to 0.75 V vs. NHE to prevent the Ru from dissolving [21]. Methanol oxidation at the sputtered electrodes was evaluated in N_2- and O_2-saturated 0.5 mol dm^{-3} H_2SO_4 + 1 mol dm^{-3} CH_3OH solutions. The measurement was conducted at the sweep rate of 10 mV s^{-1} after the pretreatment.

2.4. Electrochemical measurement of the MEA

The prepared MEA was installed in a single cell (Electrochem, Inc., EFC05-01SP) to measure its current–voltage (*i–V*) characteristics using a cell operation system (DEMO-DM0001, FC Development Co, Ltd.) in combination with a potentiostat/galvanostat (HAB-151, Hokuto Denko), and the data were collected using a datalogger (NR-2000, Keyence) (Fig. 1). Fully humidified N_2 gas was supplied to the Pt–Ru–C sputtered electrode at 50 cm^3 min^{-1} and fully humidified H_2 gas to the counter electrode at 50 cm^3 min^{-1}. Thus, a background cyclic voltammogram of the Pt–Ru–C sputtered electrode was measured. The N_2 gas was then changed to an Ar- and O_2-saturated 1 mol dm^{-3} methanol solution at the rate of 50 cm^3min^{-1} in order to compare the methanol electro-oxidation at the Pt–Ru–C sputtered electrode under the Ar and O_2 atmosphere. The cell operation system containing a pump feeds the Ar- and O_2-saturated methanol solutions from a methanol reservoir to the DMFC single cell. The methanol in the reservoir is purged by Ar and O_2 gases, so that Ar- and O_2-saturated solutions have been prepared. The exhausted methanol solution from the anode was not reused. The cell temperature was controlled at 25, 40 and 60 °C. For the voltammetry measurements, the Pt–Ru–C electrode potential was controlled versus the counter electrode, which is considered to be a dynamic hydrogen electrode (DHE). Next, the H_2 gas supplied to the counter electrode was switched to a fully humidified O_2 gas at 50 cm^3 min^{-1}. Thus, the DMFC power generation was then conducted at the cell temperatures of 25, 40 and 60 °C. During the power generation, the *i–V* and current–power (*i–P*) curves were measured by feeding an Ar- and O_2-saturated 1 mol dm^{-3} methanol solution to the anode and fully humidified O_2 gas to the cathode. All the measured currents were normalized by the geometric surface area of the Pt–Ru–C electrode, which was in contact with the polymer electrolyte membrane (5 cm^2).

3. Results and discussion

3.1. Characterization of Pt–Ru–C sputtered electrode by EDX, XRD, and XPS measurements

The SEM-EDX measurement was conducted to estimate the atomic ratio of the prepared electrodes. The obtained results are listed in Table 1. The composition of the Pt–Ru and Pt–Ru–C electrodes exhibit the highest methanol oxidation current and O_2-enhaned methanol oxidation current density [22]. The crystal structures of the Pt, $Pt_{0.78}Ru_{0.22}$, and $Pt_{0.56}Ru_{0.38}C_{0.06}$ were evaluated by XRD measurement. Pt, Pt–Ru, and Pt–Ru–C samples prepared on glass plates. For the Pt sample, three peaks corresponding to Pt (111), Pt (200), and Pt (220) are observed (JCPDS No. 04-0802), demonstrating that the sputtered Pt has a face-centered cubic (fcc) polycrystalline structure [22]. For $Pt_{0.78}Ru_{0.22}$ and $Pt_{0.56}Ru_{0.38}C_{0.06}$, the reflections also indicate the Pt fcc structure. The observed peaks are relatively small, suggesting that the crystallinity of Pt is low. The calculated values from the XRD patterns are shown in Table 2. The crystalline size of Pt decreases by the addition of C. This consideration is well supported by the TEM observations [7].

The Pt $4f_{5/2}$ and $4f_{7/2}$ binding energy are shown in Table 2 from the XPS measurement. The Pt 4f binding energy of the prepared $Pt_{0.78}Ru_{0.22}$ electrode is shifted toward a higher energy compared to that of the Pt sputtered electrode [23]. The spectrum of the $Pt_{0.56}Ru_{0.38}C_{0.06}$ electrode has almost the same binding energy as that of the $Pt_{0.78}Ru_{0.22}$ electrode. The electronic state of C 1s did not change by the addition of C. This point out no electronic interaction between the Pt and C.

3.2. Methanol oxidation selectivity at Pt–Ru–C in H_2SO_4 solution

To investigate the effect of the Ru and C addition on the methanol oxidation at the Pt electrode, the methanol oxidation voltammograms of the Pt and Pt–Ru were measured in N_2- and O_2-saturated 1 mol dm^{-3} CH_3OH + 0.5 mol dm^{-3} H_2SO_4 solutions. The obtained results are shown in Fig. 2(a) and (b), in which the dotted and solid lines represent the voltammograms in N_2 and O_2 atmospheres, respectively. For the Pt electrode, the two methanol oxidation voltammograms show that the E_{onset} is observed at 0.55 V vs. NHE under a N_2 atmosphere, which shifts to 0.66 V vs. NHE under an O_2 atmosphere. The methanol oxidation current density in the O_2 atmosphere is lower than that in the N_2 atmosphere. These results demonstrate that the methanol oxidation performance of the Pt electrode is degraded in the presence of O_2. This is because the O_2 reduction and methanol oxidation simultaneously occur at the Pt electrode under the O_2 atmosphere, which leads to the appearance of a mixed potential of the methanol oxidation and O_2 reduction in the presence of O_2 [24,25]. As a result, the methanol oxidation voltammogram of the Pt electrode in Fig. 2(a) shows a positive shift in the E_{onset} and a lower methanol oxidation current in the O_2 atmosphere.

As for the $Pt_{0.78}Ru_{0.22}$, the methanol oxidation current is enhanced and the E_{onset} shifts in the cathodic direction due to the addition of Ru in the N_2 atmosphere. These phenomena are well explained by above-mentioned methanol oxidation mechanism, in which the rate-determining step of the methanol oxidation is represented by Eq. (2) [12]. The addition of Ru to Pt accelerates the reaction of Eq. (2). When we compare the dotted and solid lines in Fig. 2(b), the methanol oxidation current in the O_2 atmosphere is smaller than that in the N_2 atmosphere. The degradation of

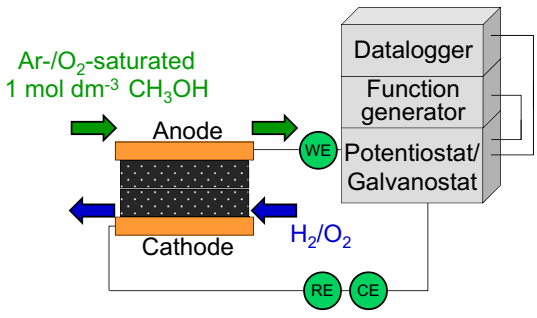

Fig. 1. Illustration of the single cell for voltammogram and power generation performance measurements.

Table 2
XRD and XPS data of Pt, Pt–Ru, and Pt–Ru–C sputtered electrodes.

Sample	2θ[a]/degree	$\beta_{1/2}$[b]/degree	Crystalline size[c]/nm	$4f_{7/2}$/eV	$4f_{5/2}$/eV
Pt	39.8	0.89	11.6	70.85	74.20
$Pt_{0.78}Ru_{0.22}$	40.2	1.48	7.0	71.31	74.62
$Pt_{0.56}Ru_{0.38}C_{0.06}$	40.4	1.74	6.0	71.38	74.68

[a] The angle of diffraction of Pt (111).
[b] The full width at half maximum of the Pt (111) peak.
[c] These values are calculated using Scherrer's equation [22].

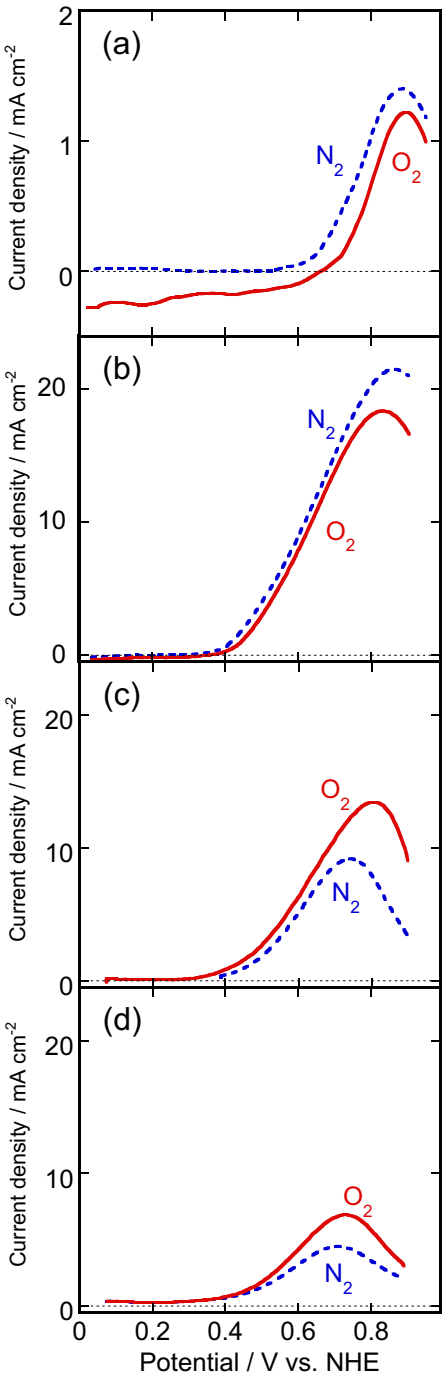

Fig. 2. Voltammograms of methanol oxidation in N_2- and O_2-saturated 0.5 mol dm^{-3} H_2SO_4 + 1 mol dm^{-3} CH_3OH solutions at sputtered electrodes of (a) Pt, (b) Pt–Ru, (c) Pt–Ru–C, and (d) Pt–Ru–C prepared on a carbon plate. Scan rate: 10 mV s^{-1}.

methanol oxidation at $Pt_{0.78}Ru_{0.22}$ in O_2 is due to the simultaneous occurrence of methanol oxidation and O_2 reduction.

The methanol oxidation voltammograms for determining the C addition effects on the Pt–Ru were measured at the $Pt_{0.56}Ru_{0.38}C_{0.06}$, which is shown in Fig. 2(c). In the figure, the E_{onset} of $Pt_{0.56}Ru_{0.38}C_{0.06}$ is the same as that of $Pt_{0.78}Ru_{0.22}$ in the N_2 atmosphere. When we compare the dotted and solid lines in Fig. 2(c), the methanol oxidation current is found to increase due to the presence of O_2. This points out that an increased number of electrons pass through the Pt–Ru–C in the presence of O_2. Therefore, methanol is electro-oxidized under O_2 atmosphere, which implies that the methanol and O_2 hardly react non-electrochemically. Moreover, the two methanol oxidation curves of $Pt_{0.56}Ru_{0.38}C_{0.06}$ show that the E_{onset} is obtained at 0.33 V vs. NHE in both the N_2 and O_2 atmospheres. These results reveal that the O_2-enhanced methanol oxidation with a comparatively negative E_{onset} is achieved by adding C to the Pt–Ru. The O_2-enhanced methanol oxidation current density is observed by the addition of C to the Pt–Ru [7,22], but that of $Pt_{0.56}Ru_{0.38}C_{0.06}$ is smaller than that of $Pt_{0.78}Ru_{0.22}$. This can be explained by the structure of Pt–Ru active site which is partially covered with C.

Fig. 2(d) shows the methanol oxidation voltammograms at the Pt–Ru–C prepared on glassy carbon. The composition of the Pt–Ru–C is presumed to be the same as that prepared on Au, because the EDX is unable to distinguish the sputtered carbon from the substrate carbon. When the methanol oxidation voltammogram of Fig. 2(c) is compared to that of Fig. 2(d), almost the same characteristics are seen in terms of the methanol oxidation current density, onset potential, and O_2-enhanced methanol oxidation. These facts indicate that the substrate does not affect the Pt–Ru–C electrocatalytic performance.

3.3. Thermal effect of methanol oxidation selectivity at Pt–Ru–C

We found that the substrate does not affect the electrocatalysis. We then investigated the thermal stability for an MEA made using post-annealing. The results of the electrochemical measurements without the post-annealing treatment are shown in Fig. 3(a). These voltammograms of solid and dotted lines were measured in O_2- and N_2-saturated 1 mol dm^{-3} CH_3OH + 0.5 mol dm^{-3} H_2SO_4, respectively. The solid line in O_2 atmosphere shows a higher methanol oxidation current than the dotted line in the N_2 atmosphere at >0.6 V vs. NHE.

Next, the prepared Pt–Ru–C electrode was post-annealed at 100, 160 °C, and the methanol oxidation activity was then measured, as shown in Fig. 3. When the methanol oxidation voltammogram for 25 °C is compared to that for 100 °C, almost the same characteristics are observed in terms of the methanol oxidation current density and O_2-enhanced methanol oxidation effect. In contrast, the O_2-enhanced methanol oxidation effect disappears in the methanol oxidation voltammogram for 160 °C.

Fig. 4 shows each current density for the methanol oxidation in O_2 and N_2 atmospheres at 0.6 V vs. NHE and the ratio of the current density ($i(O_2)/i(N_2)$) from the data of Fig. 3, and at 80, 120, 160 °C. If the ratio is higher than 1, this suggests the possibility of an O_2-enhanced methanol oxidation activity. This ratio decreases with the increasing post-annealed temperature. Finally, the O_2-enhanced methanol oxidation activity almost disappears at greater than 120 °C. The effect of the O_2-enhanced methanol oxidation is assumed to be the same mechanism as that of the Pt–C electrode. Therefore, when we assemble an MEA incorporating the sputtered Pt–Ru–C, a hot-pressing treatment should be performed at a temperature lower than 100 °C.

3.4. Methanol oxidation at Pt–Ru–C of MEA

Fig. 5 shows voltammograms of the methanol electro-oxidation measured at the Pt–Ru–C of an MEA. The Pt–Ru–C composition is assumed to be the same as that prepared on Au because carbon paper is used as a substrate. The voltammogram measurements were conducted by feeding Ar- and O_2-saturated 1 mol dm^{-3} methanol to the Pt–Ru–C and humidified H_2 to the counter electrode by changing the cell temperature. The inset in Fig. 5 is a background cyclic voltammogram of the Pt–Ru–C measured under a humidified N_2 atmosphere at 25 °C. From the voltammogram, the

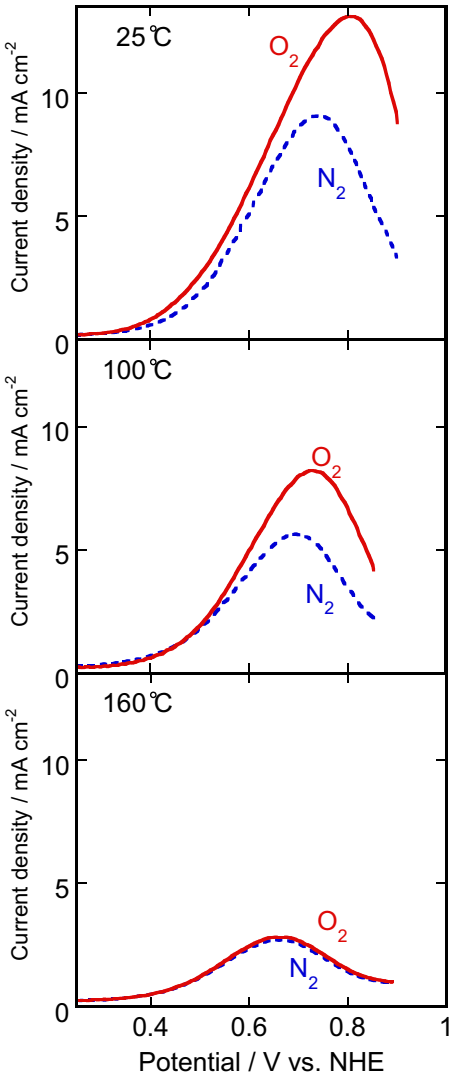

Fig. 3. Voltammograms of methanol oxidation reaction under O_2- and N_2-saturated 0.5 mol dm^{-3} H_2SO_4 + 1 mol dm^{-3} CH_3OH solutions at Pt–Ru–C electrode at 25, 100, and 160 °C. Scan rate: 10 mV s^{-1}.

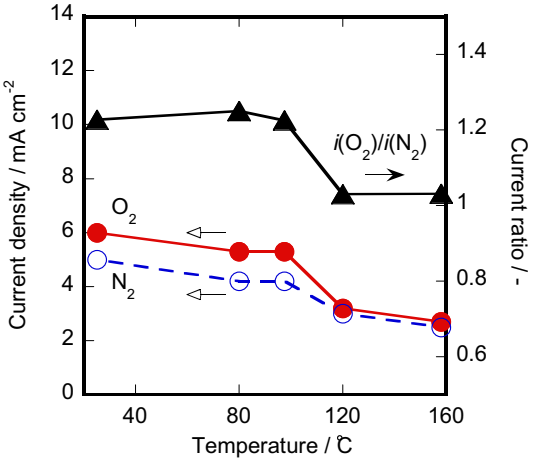

Fig. 4. Annealing temperature dependence of methanol oxidation current at 0.6 V vs. RHE in O_2- and N_2-saturated 0.5 mol dm^{-3} H_2SO_4 + 1 mol dm^{-3} CH_3OH solutions, and the methanol oxidation current ratio. The electrochemical measurements were carried out at 25 °C.

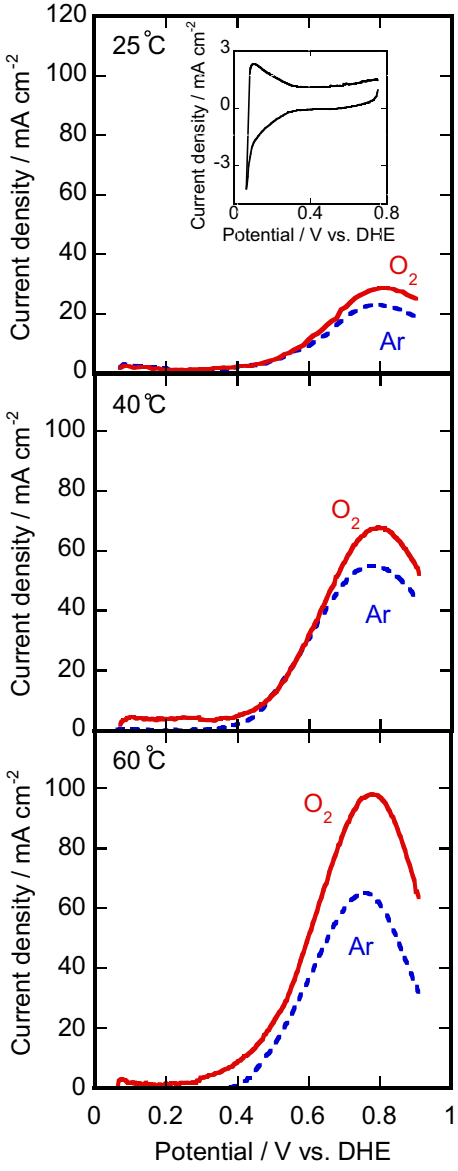

Fig. 5. Current–potential curves of methanol oxidation at Pt–Ru–C electrode of an MEA installed in a single cell. Measurements were conducted at 25, 40, and 60 °C by feeding Ar- and O_2-saturated 1 mol dm^{-3} CH_3OH solution to the anode and humidified H_2 gas to the counter electrode. Scan rate: 50 mV s^{-1}.

electrical double layer capacitance was estimated in a potential region of 0.3–0.7 V vs. DHE [14]. This suggests that the electrochemical surface area of the Pt–Ru–C prepared on the Au and the carbon paper are presumed to be at the same level.

In Fig. 5, the methanol oxidation at 25 °C is enhanced by the dissolved O_2 even in the MEA system. This implies that the O_2-enhanced methanol oxidation takes place at the Pt–Ru–C/Nafion membrane system in the same way as in the H_2SO_4 solution system. The magnitude of the methanol oxidation current is almost the same as that observed in the H_2SO_4 solution. This is thought to be due to the same electrochemical surface areas of the Pt–Ru–C prepared on the Au and on the carbon paper. In Fig. 5, methanol oxidation voltammograms obtained at 40 and 60 °C are also plotted. In each case, the methanol oxidation is clearly improved by the added O_2. Under the Ar atmosphere, the methanol oxidation current increases according to an increase in the cell temperature,

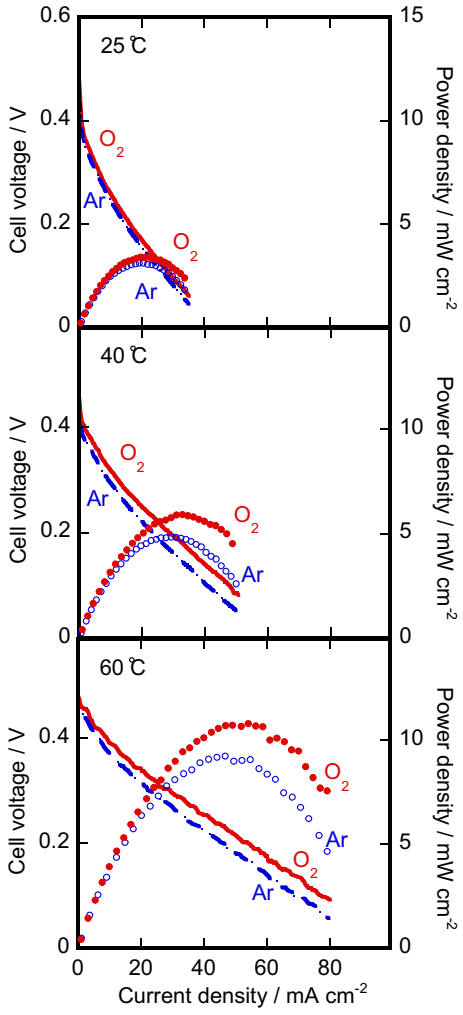

Fig. 6. Current–voltage and current–power characteristics of a DMFC single cell incorporating an MEA which has a sputtered Pt–Ru–C anode catalyst layer. Symbols denote the power density. Measurements were conducted at 25, 40, and 60 °C by feeding Ar- and O_2-saturated 1 mol dm^{-3} CH_3OH solution to the anode and humidified O_2 gas to the cathode.

while, under O_2, the E_{onset} is cathodically shifted and the methanol oxidation current increases.

3.5. Direct methanol fuel cell power generation in a single cell incorporating the MEA

The cathode gas was then switched to a humidified O_2 gas. The DMFC single cell performances were then measured by feeding an Ar- and O_2-saturated 1 mol dm^{-3} methanol solution to the anode. Fig. 6 shows the single cell performances regarding the *i*–*V* and *i*–*P* characteristics measured at 25, 40, and 60 °C, respectively. These results show that the methanol oxidation and its O_2-enhancement are accelerated by the cell temperature.

These results agreed well with the results shown in Fig. 5. Therefore, it is found that the prepared Pt–Ru–C sputtered electrode is strongly expected to be a suitable DMFC anode catalyst for feeding the methanol and O_2 mixture.

4. Conclusions

We successfully prepared useful Pt–Ru–C electrodes using a multi-target sputtering system for the DMFC anode. The obtained electrode possesses an O_2-enhanced methanol performance and a reaction selectivity for the methanol oxidation under an O_2 atmosphere. It is confirmed that the O_2-enhanced methanol oxidation effect remains up to a 100 °C heat treatment. Therefore, a single DMFC cell was assembled incorporating the 100 °C hot-pressed MEA containing the Pt–Ru–C electrode. Finally, the O_2-enhanced methanol oxidation activity was clearly observed at the Pt–Ru–C of the single DMFC cell. The presented Pt–Ru–C electrode can be used as an efficient DMFC anode by feeding the methanol and O_2 mixture.

Acknowledgment

The present work was supported by a Grant-in-Aid for Scientific Research (No. 24350091) from the Japan Society for the Promotion of Science (JSPS, Japan).

References

[1] J. Kawaji, S. Suzuki, Y. Takamori, M. Morishima, Electrochim. Acta 55 (2010) 8018–8022.
[2] P. Liu, G.P. Yin, C.Y. Du, Electochem. Commun. 10 (2008) 1471–1473.
[3] H. Liu, C. Song, L. Zhang, J. Zhang, H. Wang, D.P. Wilkinson, J. Power Sources 155 (2006) 95–110.
[4] X. Ren, P. Zelenay, S. Thomas, J. Davey, S. Gottesfeld, J. Power Sources 86 (2000) 111–116.
[5] Y. Ando, K. Sasaki, R. Adzic, Electrochem. Commun. 11 (2009) 1135–1138.
[6] V.B. Oliveira, C.M. Rangel, A.M.F.R. Pinto, Int. J. Hydrogen Energy 34 (2009) 6443–6451.
[7] M. Umeda, K. Nagai, M. Shibamine, M. Inoue, Phys. Chem. Chem. Phys. 12 (2010) 7041–7049.
[8] H.A. Gasteiger, N. Marković, P.N. Ross Jr., E.J. Cairns, J. Phys. Chem. 97 (1993) 12020–12029.
[9] A. Kabbabi, R. Faure, R. Durand, B. Beden, F. Hahn, J.-M. Leger, C. Lamy, J. Electroanal. Chem. 444 (1998) 41–53.
[10] H.N. Dinh, X. Ren, F.H. Garzon, P. Zelenay, S. Gottesfeld, J. Electroanal. Chem. 491 (2000) 222–233.
[11] C. Bock, B. MacDougall, Y. LePage, J. Electrochem. Soc. 151 (2004) A1269–A1278.
[12] M. Umeda, M. Kokubo, M. Mohamedi, I. Uchida, Electrochim. Acta 48 (2003) 1367–1374.
[13] M. Umeda, H. Ojima, M. Mohamedi, I. Uchida, J. Power Sources 136 (2004) 10–15.
[14] M. Umeda, H. Sugii, I. Uchida, J. Power Sources 179 (2008) 489–496.
[15] S. Tanaka, M. Umeda, H. Ojima, Y. Usui, O. Kimura, I. Uchida, J. Power Sources 152 (2005) 34–39.
[16] M. Umeda, K. Sayama, M. Inoue, J. Renew. Sustain. Energy 3 (2011) 043107.
[17] M. Inoue, T. Iwasaki, M. Umeda, Electrochemistry 79 (2011) 329–333.
[18] G.J. Janz, in: D.J.G. Ives, G.J. Janz (Eds.), Reference Electrode Theory and Practice, Academic Press, New York and London, 1961 (chapter 4).
[19] M. Umeda, T. Maruta, M. Inoue, A. Nakazawa, J. Phys. Chem. C 112 (2008) 18098–18103.
[20] M. Umeda, Y. Kuwahara, A. Nakazawa, M. Inoue, J. Phys. Chem. C 113 (2009) 15707–15713.
[21] T.J. Schmidt, M. Noeske, H.A. Gasteiger, R.J. Behm, P. Britz, H. Bönnemann, J. Electrochem. Soc. 145 (1998) 925–931.
[22] M. Umeda, Y. Matsumoto, M. Inoue, S. Shironita, J. Electrochim. Acta 101 (2013) 142–150.
[23] L. Giorgi, A. Pozio, C. Bracchini, R. Giorgi, S. Turtù, J. Appl. Electrochem. 31 (2001) 325–334.
[24] W. Vielstich, V.A. Paganin, F.H.B. Lima, E.A. Ticianelli, J. Electrochem. Soc. 148 (2001) A502–A505.
[25] L. Colmenares, E. Guerrini, Z. Jusys, K.S. Nagabhushana, E. Dinjus, S. Behrens, W. Habicht, H. Bönnemann, R.J. Behm, J. Appl. Electrochem. 37 (2007) 1413–1427.